ASTRONOMY & ASTROPHYSICS
SUPPLEMENT SERIES

Astron. Astrophys. Suppl. Ser. **59,** 511-521 (1985)

High resolution radio observations of low luminosity radio galaxies

P. Parma ([1,2]), R. D. Ekers ([1]) and R. Fanti ([2,3])

([1]) NRAO, VLA Site, Socorro, U.S.A.
([2]) Istituto di Radioastronomia del CNR, via Irnerio 46, 40126 Bologna, Italy
([3]) Dipartimento di Astronomia, Universita' di Bologna, Italy

Received July 24, accepted November 5, 1984

Summary. — New maps for seven low luminosity radio galaxies, obtained with the Westerbork Synthesis Radio Telescope (WSRT) at the frequencies of 0.6, 1.4 and 5.0 GHz are presented here. For two of them a VLA map at 1.4 GHz, with a resolution of about 3″, is also given.
Two, possibly three, of the sources show radio structures of the Head-Tail or Wide-Angle-Tail type. Two others show pronounced S (or rotational type) distortions.

Key words : radiogalaxies.

1. Introduction.

This paper is one of a series of papers on radio properties of low luminosity radio galaxies selected from identifications of radio sources of the B2 catalogue with bright galaxies (see Colla *et al.* (1975a, b) and Fanti *et al.* (1978) for the selection criteria of the samples).

Ekers *et al.* (1981) presented a discussion of the radio properties of a complete sub-sample of 17 of these radio galaxies with linear sizes > 50 kpc and $\log P_{408} < 25.0$ (W/Hz). In order to extend the analysis to a larger sample, we are carrying on new observations with both the WSRT and the VLA.

We present here new WSRT radio data on seven sources, from the above samples, not mapped before with the present resolution and sensitivity.

The sources were chosen because of their unusual radio morphology, as it appeared on lower quality maps produced by means of short observations at different hour angles with the WSRT (Fanti *et al.*, 1978).

For two of them also 1.4 GHz VLA maps, with a resolution of $\sim$ 3 arcsec, are shown.

2. Observations and data reduction.

The observations were made with the WSRT at 4995 and/or 1415 and 610 MHz. All but B2 0915+32 and B2 1116+28 at 5 GHz and B2 0828+32 at 0.6 GHz were mapped before the extension of the Westerbork array to 3 km. The details of the WSRT observations are given in table I. The WSRT system is described by Weiler (1973), Baars and Hooghout (1974) and Hogbom and Brouw (1974).

Send offprint requests to : R. Fanti.

The data reduction was done at the University of Groningen with the GIPSY interactive programs described by Shostak and Allen (1979) and/or with the AIPS package at the VAX 11/780 of the CNR, in Bologna. After the visibility data were transformed into total and polarized intensity, the CLEAN algorithm was applied. The dirty maps were CLEANed until the sum of the CLEAN component flux densities showed convergence. At this stage the « residual maps » were consistent with the expected instrumental noise. Flux densities were determined by integration of the CLEANed map brightness over a box enclosing the extended source.

The VLA maps of B2 1430+25 and B2 1827+32 were obtained as a part of a VLA program aimed at mapping all the radio galaxies of the two samples (Parma *et al.*, in preparation).

Tables II, III and IV present the observational data and table V gives some intrinsic source parameters (assuming $H_0 = 100$ km/(s Mpc)). Internal energy ($U_{\min}$) and energy density ($u_{\min}$) are determined by using the equipartition assumption with standard formulae (e.g. Pacholczyk, 1970). It is assumed that : a) the radio spectra are power laws from 10 MHz to 100 GHz ; b) equal energies reside in relativistic electrons and protons. The radiating volumes are approximated with ellipsoids with the major axis on the plane of the sky and a filling factor of 1. Owing to the uncertainties in the above assumptions, the equipartition parameters have to be taken as order of magnitude estimates.

3. Results.

B2 0828+32

This radio source has a prominent distorted structure of the rotational type, as found in other radio galaxies,

e.g. : 3C 315 and 3C 192 (Hogbom, 1979), NGC 326 (Ekers *et al.*, 1978), 4C 48.29 (van Breugel and Jagers, 1982). Maps of the total intensity and polarization are shown in figures 1a and 1b at 1.4 GHz and in figures 2a and 2b at 0.6 GHz.

A hot spot is visible, at the present resolution, in the western component. Higher resolution observations at 5 GHz with the WSRT (Feretti *et al.*, 1983), confirm the existence of this hot spot, while they do not show any bright feature in the eastern lobe.

A comparison of the 1.4 GHz map with that at 0.6 GHz, allows the study of the spectral index distribution across the source. The two main components have a rather constant spectrum ([1]), with $\langle \alpha \rangle \sim 0.7$ ($\pm$ 0.05) in the western lobe and ~ 0.65 ($\pm$ 0.05) in the eastern one. On the contrary the two low brightness extensions (wings) towards north and south have very steep spectra $\langle \alpha \rangle \sim 1.2 - 1.4$ ($\pm$ 0.1) in the southern and $\gtrsim 1.2$ ($\pm$ 0.2) in the northern one. No significant spectral gradients are seen within them.

The source is highly polarized at both frequencies. Although the surface brightness in the northern wing is too low at 1.4 GHz to measure any significant polarization, at 0.6 GHz the brightness sensitivity is sufficient to detect significant polarization. Typical values of percentage polarization are up to 20-30 % all over the source. There is no indication of depolarization between the two frequencies.

Comparison of the polarization angle at the two frequencies shows that the rotation angle $\theta_{50} - \theta_{21}$ is $\sim 120 \pm 5$ deg and very uniform across the whole source. Ambiguities of $n\pi$ can be excluded by using the 5.0 GHz data by Feretti *et al.* (1983). The rotation measure is 10.7 rad/sq.m. A map of the projected magnetic field, superimposed on the 0.6 GHz map, is given in figure 2c.

The distribution of the polarized emission and the orientation of the magnetic field in the western component (perpendicular to the lobe axis) suggest the presence of a jet, characterized by a perpendicular field, pointing towards the hot spot and partially masked by the diffuse emission of the lobe.

The morphology displayed by this source is suggestive of a change in orientation of the central engine that is powering the external lobes (e.g. Miley, 1976). Whether such a change has occurred at a regular rate, as due to a precession phenomenon in a way similar to that suggested for NGC 326 (Ekers *et al.*, 1978b) is unclear (although not impossible). Differently from NGC 326, where the ridge of extended emission runs continuously with moderate curvature from the « young lobes » to the « old » ones and is accompanied by a gradual steepening of the spectrum, in the present case the change of orientation is sharper, giving the impression of a cross-shaped source, and no gradual steepening of the radio spectrum is evident. The source morphology might be due to an abrupt change in the source ejection axis, but might also be reconciled with a precession phenomenon by taking an appropriate orientation of the axis of the precession cone (e.g. an angle of 60 deg between the line of sight and the precession cone axis and a half opening angle of $\sim$ 25 deg). The lack of evidence for a regular steepening in the radio spectrum from the « young » to the « old » lobes, which would provide information on the particles lifetime, prevents from constraining dynamical models for the orientation change.

In 3C 315, NGC 326 and 4C 48.29, which display similar S-type distortions, the parent galaxy belongs to a double system. Tidal interaction has been suggested as responsible for the change of the ejection direction as a consequence of a torque exerted by the companion galaxy on the gaseous halo which recollimates the beam supplying the lobes (Wirth *et al.*, 1982). The present galaxy has no visible companion on the PSS prints.

B2 0843+31

The total intensity map at 1.4 GHz, is shown in figure 3. The source consists of three components, with an overall size of $\sim 4'$. The southern component is unresolved at our resolution, while the two others (indicated by « A » in Fig. 3 and table II) are partially blended. The galaxy suggested as identification is $\sim$ 30 arcsec south of the peak of the central component, which is mid-way between the southern and the northernmost component.

The two northern components are polarized up to 14 %. The peak of the polarized radiation lays in between them. The p.a. of the electric vector changes by more than 70 deg across the two components. The southern component does not show any significant polarization.

At present it is unclear whether the association of the whole source with the galaxy is correct. Higher resolution observations are needed to clarify the nature of the source.

B2 0915+32

A WSRT map at 1.4 GHz ($24'' \times 45''$ resolution) was presented by Ekers *et al.* (1981) (see also Fomalont and Bridle, 1978a). The source is very extended ($\sim$ 10 arcmin, corresponding to 500 kpc). Its main characteristic at low resolution is the presence of two bright resolved regions, some 3 arcmin apart, roughly symmetric with respect to the galaxy, from which more emission of lower brightness extends outwards, trailing gradually into the noise.

The new map presented here (Fig. 4), with $4'' \times 7''$ resolution at 5 GHz, allows us to study the inner part of the source, between the two bright regions. It shows an unresolved core, coinciding with the nucleus of the parent galaxy and a twin jet of very low brightness. The twin jet terminates in the two bright regions of the 1.4 GHz map.

The jet shows two peculiar characteristics. The first is an antisymmetric (or S-type) change of p.a., by more than 40 degrees, occurring within 6″ from the core. Second, at $\sim$ 40″ from the core, the northern jet bends again by $\sim$ 30 deg, while the southern one also curves but not as much. The northern jet, with its strong curvature at $\sim$ 40″ of the core, is remarkably similar to that of 3C 31. However this source shows both types of symmetry : the rotational symmetry within 6″ from the core ($<$ 6 kpc) and the mirror symmetry at a larger distance ($\sim$ 35 kpc), visible in the 1.4 GHz map. In this respect it recalls some head-tail sources (e.g. 3C 129, Rudnick and Burns, 1981) which

([1]) $S(\nu) \propto \nu^{-\alpha}$.

have been modelled as swept-back precessing jets (Icke, 1981).

The parent galaxy belongs to a visual double system, possibly a physical pair, with a projected separation of $\sim$ 30 kpc. It is tempting to ascribe the jet distortions to the presence of the companion galaxy, according to the models described by Blandford and Icke (1978) or Wirth *et al.* (1982).

B2 1116+28

The source is a wide angle tail (WAT) (Fig. 5a) and it is identified with a 14.3 magnitude elliptical galaxy projected onto the Zwicky cluster 11 15.2+30 13 (Near, Medium Compact), which contains the Abell cluster A 1213 with $z = 0.0484$. The galaxy associated with the radio source is a double system with a redshift ($z = 0.0667$) different from both that of A 1213 and that of a Near Zwicky cluster. Therefore, as far as it is known at present, this appears to be an isolated galaxy.

At 4995 MHz (Fig. 6) only the central component is mapped at 4×8 arcsec resolution. It consists of a bright core plus a symmetric low brightness emission in p.a. $\sim$ 100 deg, possibly a twin jet, slightly bent northward in the same way as the larger scale emission.

Appreciable polarization is present at 1415 MHz (Fig. 5b). The maxima of both the polarized radiation and of the fractional polarization coincide with the peaks of the total intensity. Components A and C have higher polarization than component B.

We have used the WSRT maps at the two frequencies, cleaned and restored with identical Gaussian beams, to derive the spectral index distribution in the source. The spectral index is $\sim$ 0.7 ($\pm$ 0.05) in the central component and $\sim$ 1.4 ($\pm$ 0.2) in the two outer lobes.

Comparison of the polarization maps at the two frequencies, convolved to the same resolution, shows no evidence for depolarization in component C, which is the only component with detected polarization at 5 GHz. The rotation angle $\theta_{21} - \theta_6$ in component C is $\sim$ 12 deg, corresponding to a rotation measure of 21 rad/sq.m. (assuming no $n\pi$ ambiguity). Assuming this value for the rotation measure, the difference between the p.a. at 5 GHz and the intrinsic one is negligible. The p.a. of the magnetic field would be $\sim$ 0, so that the field would be perpendicular to the jet axis.

B2 1430+25

Short observations at 1.4 GHz of this radio galaxy (Fanti *et al.*, 1978) showed only a barely resolved source with the galaxy located at the southern edge of the radio isophotes, resembling a small head-tail source.

Fomalont and Bridle (1978b), mapped the source at 2.7 GHz with the NRAO interferometer. In their map the source is resolved into a small double, apparently unrelated to the galaxy.

We have reobserved the source with the WSRT at 5 GHz with a resolution of 7×16 arcsec (Fig. 7a) and with the VLA at 1.4 GHz with a resolution of $\sim$ 3 arcsec (Fig. 7b) (Parma *et al.*, in preparation).

Although in the WSRT map the source looks indeed like a small double with an incorrect identification, the VLA map supports the head-tail interpretation. The southern component looks much like an « arrow head », the galaxy sitting on its tip. The base of the « arrow head » is definitely widened ($\sim$ 15″) and from close to one of its vertices a long and collimated structure emerges, the « stick » of the arrow, ending in a point-like bright component, the « notch ».

Convolving the VLA map to the resolution of the WSRT 5 GHz map, a spectral comparison can be performed. The « arrow head » and the « stick » have rather steep spectra, $\alpha \sim 1.2$ to 1.7 ($\pm$ 0.10) respectively, while the northern component has $\alpha \sim 1.0$ ($\pm$ 0.05).

The « notch » appears different from the rest of the « arrow » also for the polarization characteristics. It is less polarized, but it does not show any depolarization between the two frequencies ($\sim$ 10 % at both). The « arrow head », on the contrary is $\sim$ 18 % polarized at 5 GHz and only $\sim$ 6 % at 1.4 GHz. The rotation angles are significantly different : $\theta_{21} - \theta_6 \sim -82$ deg in the northern component, $\sim +12$ deg in the « arrow head ». Owing to its different properties, the « notch » could be a background source.

Were it not for the relative position of the galaxy with respect to the radio source, this could also be a classical high radio luminosity double, with emission bridges between the lobes. Clearly higher resolution observations of the « arrow head » are needed to definitely confirm the « head-tail » nature of the source.

The galaxy does not appear to be associated with any evident cluster or group of galaxies.

A second optical object in the field, noted by Fomalont and Bridle, very red and fainter, possibly a galaxy as well (marked in Fig. 7), seems definitely unrelated to the source.

B2 1637+29

B2 1637+29 is one of the most peculiar sources of the sample. The total intensity map (Fig. 8a) shows an almost circular structure with a deep central hole. A WSRT map at 5 GHz, produced by means of short observation (Feretti *et al.*, 1983) revealed an unresolved core coinciding with the galaxy's nucleus and a jet-like feature pointing to a bright region corresponding to region B of the 1.4 GHz map. Therefore the source appears as a twin head-tail, in which the two trails coalesce (for a similar case see, e.g., B2 1502+28, Valentijn, 1981).

Significant polarization has been found only in region B.

We have undertaken a detailed study of this source at two frequencies (1.4 and 5.0 GHz) using the VLA. Preliminary results of this study confirm the head-tail structure of the source.

From an inspection of the PSS prints, the galaxy associated with this radio source does not appear to belong to any evident cluster or group of galaxies. The source is projected onto the Zwicky cluster 16 35.9+29 39 (Near) but the redshift of the associated galaxy ($z = 0.0875$) is too high for a Near cluster.

B2 1827+32

Maps of the total intensity and polarization are given in figure 9a-b. The source has a triple structure, distorted and rather asymmetric. Component C is relatively compact

and about 3 times brighter than component A which is more extended. The weak source North of component A might be a background source, not related to 1827+32. Component B, which is slightly resolved, coincides in position with the nucleus of the galaxy.

Only small regions of both A and C show significant polarization, while the central component B is unpolarized.

A VLA map at 1.4 GHz of component B, with 3 arcsec resolution is presented in figure 9c (from Parma *et al.*, in preparation). Component B is well resolved here in a compact core, accounting for most of the flux, and two symmetric, much fainter, jets. The jets are oriented ~ 70 deg so there must be a change in p.a. going from the core to the outer components of more than 60 degrees.

4. Conclusions.

4.1 Occurrence of jets in radio galaxies. — At least three of the sources presented here show evidence for jets (B2 0915+32, B2 1116+28, B2 1827+32). One of them belongs to the complete sample of 17 low luminosity radio galaxies with linear size larger than 50 kpc, studied by Ekers *et al.* (1981). This increases the number of the sample members with jets to 10, out of the 12 sources studied with enough resolution to see jets if present.

4.2 Head-tail and wide-angle tail sources. — Most of the known head-tail and wide-angle tail radio sources are found in radio surveys of Abell clusters. There are however sources of this morphological type, which belong to less rich aggregates of galaxies (e.g., B2 1615+35, Ekers *et al.*, 1978a) or lay in regions of space of very low galaxies density (e.g. B2 0800+24, Stocke and Burns, private communication ; Burns, 1983). The present observations have revealed two new sources of this type (B2 1116+28 and B2 1637+29), plus a possible third one (B2 1430+25), which do not appear to belong to rich clusters or to groups of galaxies.

It is worth mentioning that in the B2 samples of radio galaxies, which are unbiased for cluster membership, head-tail and wide-angle tail sources are about equally divided between Abell and non-Abell cluster members. The membership to less rich galaxy aggregates is difficult to ascertain and will require more optical work.

4.3 Large scale S-type distortions. — Two sources of the sample (B2 0828+32 and B2 1827+32) show large scale S type distortions, suggestive of precession phenomena of the central engine. It is emphasized that in the case of B2 0828+32 the brightness ratio between the « young lobes » and the « old wings » is about 100 to 1. This stresses that high sensitivity, high dynamic range observations are necessary to find radio features of this type and to properly evaluate their occurrence in complete samples of radio sources.

Acknowledgements.

We thank the staff of the Westerbork Radio Telescope and the Reduction Group for their work on the observations. We also thank R. Primavera for preparing the figures.

We acknowledge an anonymous referee for several comments which improved the presentation of the paper.

The Westerbork Radio Observatory is operated by the Netherlands Foundation for Radio Astronomy with the financial support of the Netherlands Organization for the Advance of Pure Research. The National Radio Astronomy Observatory is operated by Associated Universities, Inc. under contract with the National Science Foundation.

References

Baars, J. W. M., Hooghout, B. G. : 1974, *Astron. Astrophys.* **31,** 323.
Blandford, R. D. and Icke, V. : 1978, *Monthly Notices Roy. Astron. Soc.* **169,** 395.
Burns, J. : 1983, Proc. of the workshop on *Astrophysical Jets,* ed. by Ferrari and Pacholczyk (Reidel) p. 67.
Colla, G., Fanti, C., Fanti, R., Gioia, I., Lari, C., Lequeux, J., Lucas, R., Ulrich, M. H. : 1975a, *Astron. Astrophys. Suppl. Ser.* **20,** 1.
Colla, G., Fanti, C., Fanti, R., Gioia, I., Lari, C., Lequeux, J., Lucas, R. and Ulrich, M. H. : 1975b, *Astron. Astrophys.* **38,** 209.
Ekers, R. D., Fanti, R., Lari, C., Ulrich, M. H., 1978a, *Astron. Astrophys.* **69,** 253.
Ekers, R. D., Fanti, R., Lari, C., Parma, P. : 1978b, *Nature* **276,** 588.
Ekers, R. D., Fanti, R., Lari, C., Parma, P. : 1981, *Astron. Astrophys.* **101,** 194.
Fanti, R., Gioia, I., Lari, C., Ulrich, M. H. : 1978, *Astron. Astrophys. Suppl. Ser.* **34,** 341.
Feretti, L., Giovannini, G., Gregorini, L., Parma, P. : 1983, *Astron. Astrophys.* **126,** 311.
Fomalont, E. B., Bridle, A. H. : 1978a, *Astrophys. J.* **223,** L9.
Fomalont, E. B., Bridle, A. H. : 1978b, *Astron. J.* **83,** 725.
Hogbom, J. A., Brouw, W. N. : 1974, *Astron. Astrophys.* **33,** 289.
Hogbom, J. A. : 1979, *Astron. Astrophys. Suppl. Ser.* **36,** 173.
Icke, V. : 1981, *Astrophys. J.* **246,** L65.
Miley, G. K. : 1976, *Physics of non thermal radio sources,* Proceedings of Nato Summer School, ed. by Setti (Reidel) p. 1.
Pacholczyk, A. G. : 1970, *Radio Astrophysics* (W. H. Freeman and Co).
Rudnick, L. and Burns, J. O. : 1981, *Astrophys. J.* **246,** L69.
Shostak, G. S., Allen, R. J. : 1980, Proceeding of the ESO workshop *Two dimensional photometry,* ed. by P. Crane and K. Kjar.
Valentijn, E. A. : 1981, *Astron. Astrophys.* **102,** 53.
Van Breugel, W. and Jagers, W. : 1982, *Astron. Astrophys. Suppl. Ser.* **49,** 529.
Weiler, K. W. : 1973, *Astron. Astrophys.* **26,** 403.
Wirth, A., Smarr, L., Gallagher, J. S. : 1982, *Astron. J.* **87,** 602.

TABLE I. — *WSRT observational parameters.*

Source B2 Name	Obs. frequency GHz	Obs. data Year	Obs. data Day	Obs. time hours	Interf. spacing short./increm./long. meters	HPBW arcsec	r.m.s. noise mJy/beam
0828+32	1.4	77	240	12	54 / 72 / 1422	25 x 47	0.8
	0.6	83	29	12	54 / 72 / 2736	25 X 47	1.2
0843+31	1.4	77	255	12	54 / 72 / 1422	25 x 48	0.4
0915+32	5.0	81	123	12	54 / 72 / 2736	4 / 7	0.3
1116+28	1.4	77	332	12	72 / 72 / 1440	24 x 53	0.5
	5.0	81	124	12	54 / 72 / 2736	4 x 8	0.4
1430+25	5.0	77	107	12	72 / 72 / 1440	7 x 16	0.9
1637+29	1.4	77	254	12	54 / 72 / 1422	25 x 50	0.4
1827+32	1.4	77	235	12	54 / 72 / 1422	25 x 47	0.5

TABLE II. — *Observational data at 1.4 GHz.*

Source B2 Name	m v	S(1.4) mJy	Angular size arcsec	Polarized flux mJy	Fractional polar. %	P.A. degrees
0828+32	15.8	1853	420			
A		66	~ 240			
B		817	100 x 70	73	9	-34
C		88	~ 200	22	25	-9
D		883	100 x 70	28	3	121
0843+31	16.5	126	216			
A		71	120 x 43	4	5	2
B		55	< 10	< 2	< 4	
1116+28	14.3	440	300 x 124			
A		134	105 x 124	12	9	49
B		133	148 x 91	4	3	125
C		199	18 x < 53	11	6	105
1637+29	14.8	312	220 x 200			
A		66	110 x 90		< 2	
B		213	150 x 60	13	6	29
1827+32	15.1	302	440			
A		74	180 x 35	5	7	-3
B		57	50 x 40	2	3	44
C		141	90 x 80	1	< 1	35

TABLE III. — *Observational data at 5.0 GHz.*

Source B2 Name	m v	S(5.0) mJy	Angular size arcsec	Polarized flux mJy	Fractional polar. %	P.A. degrees
0915+32	14.5					
Core		12	< 2			
Twin jet		10	60			
A (north)		21	25x15			
B (south)		64	50x20			
1116+28	14.3					
A		> 12				
Core		30	4 (p.a. 90)			
Twin jet		50	45	5	7	93
B		> 11				
1430+25	15.7	103	90			
A		65	17 x 32	11	18	30
B		38	11 x 17	4	10	35

TABLE IV. — *Observational data of B2 0828+32 at 0.6 GHz.*

Radio Component	S(0.6) (mJy)	Angular Size arcsec	Polarized Flux mJy	Fractional Polarization %	P.A. of Pol. deg.
D (West)	1670	100x70	91	5	49
B (East)	1360	100x70	156	12	93
A (North)	230	300x100	34	15	49
C (South)	370	300x150	61	17	98

TABLE V. — *Intrinsic properties.*

Source B2 Name	z	M_v	Log P (Watt/Hz)	D (kpc)	u_{min} (E-13 erg/cm^3)	U_{min} (E57 ergs)
0828+32	.051	-21.2	24.71	319		
D,B					8.0	6
A,C					0.7	4
0843+31	.067	-20.2	23.53	216		
A					3.0	2
B						
0915+32	.062	-21.9	24.00	500		
Jets					50.	0.04
A					20.	0.3
B					30.	0.9
1116+28	.067	-22.3	24.33	300		
Jets						
A,B					1.6	5
1430+25	.081	-21.3	24.35	110		
A					40.	1
B					80.	0.4
1637+29	.088	-22.8	24.41	347		
A					0.6	5
B					1.6	8
1827+32	.066	-22.3	24.15	435		
A					3.0	2
B					4.5	1
C					2.3	4

Key to table V

z Redshift
M_v Absolute visual magnitude
Log P Logarithm of monochromatic power at 1.4 GHz
D Largest projected size
u_{min} Range of values of equipartition energy density
U_{min} Total equipartition energy

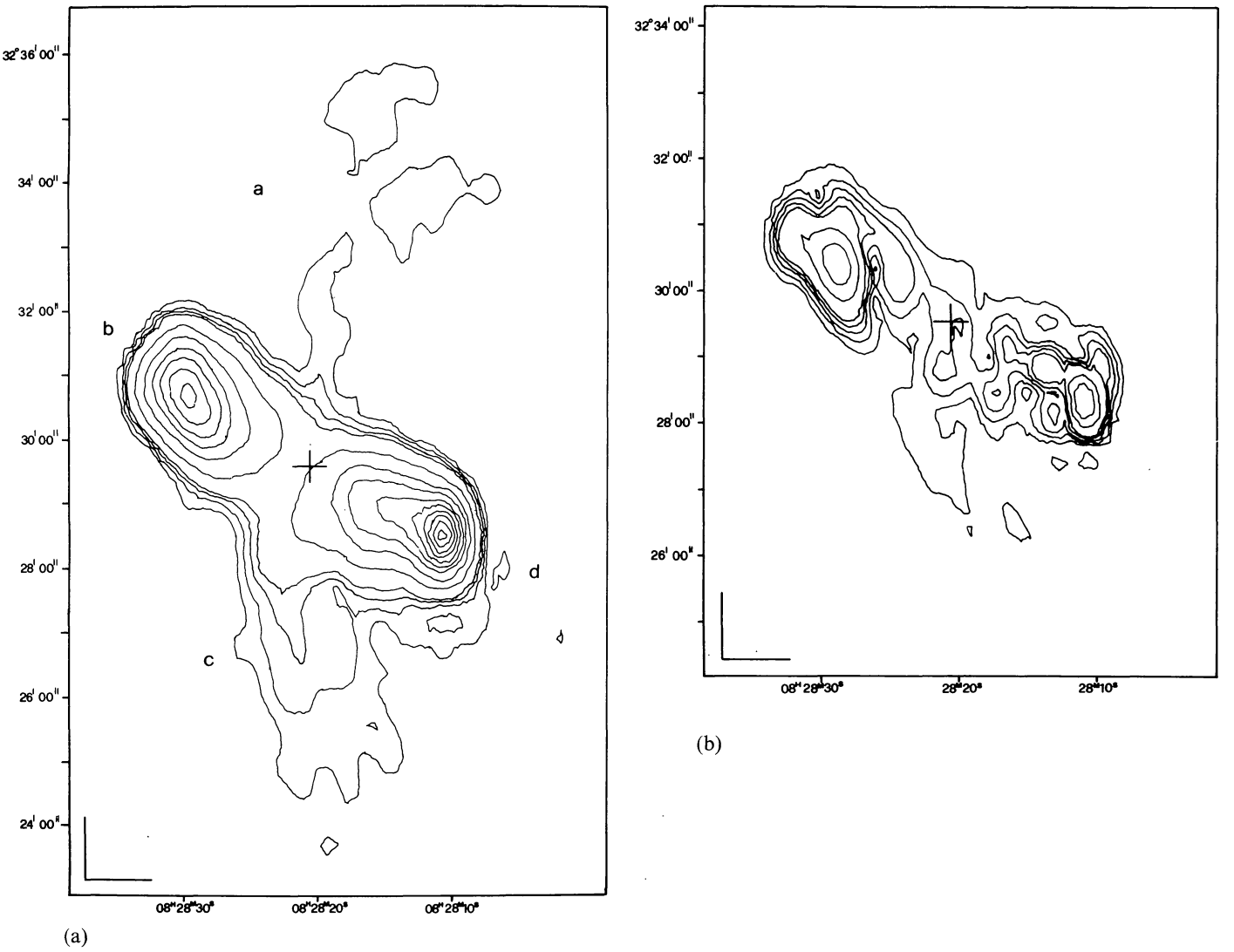

FIGURE 1. — The brightness distribution of B2 0828+32 at 1.4 GHz. The cross marks the position of the galaxy's center. (a) The total intensity map ; contours are : 2.5, 5, 10, 15, 30, 45, 60, 100, 125, 150, 175, 200, 225 mJy/beam. (b) The polarized intensity map ; contours are : 2, 4, 6, 8, 10, 20, 30, 40 mJy/beam.

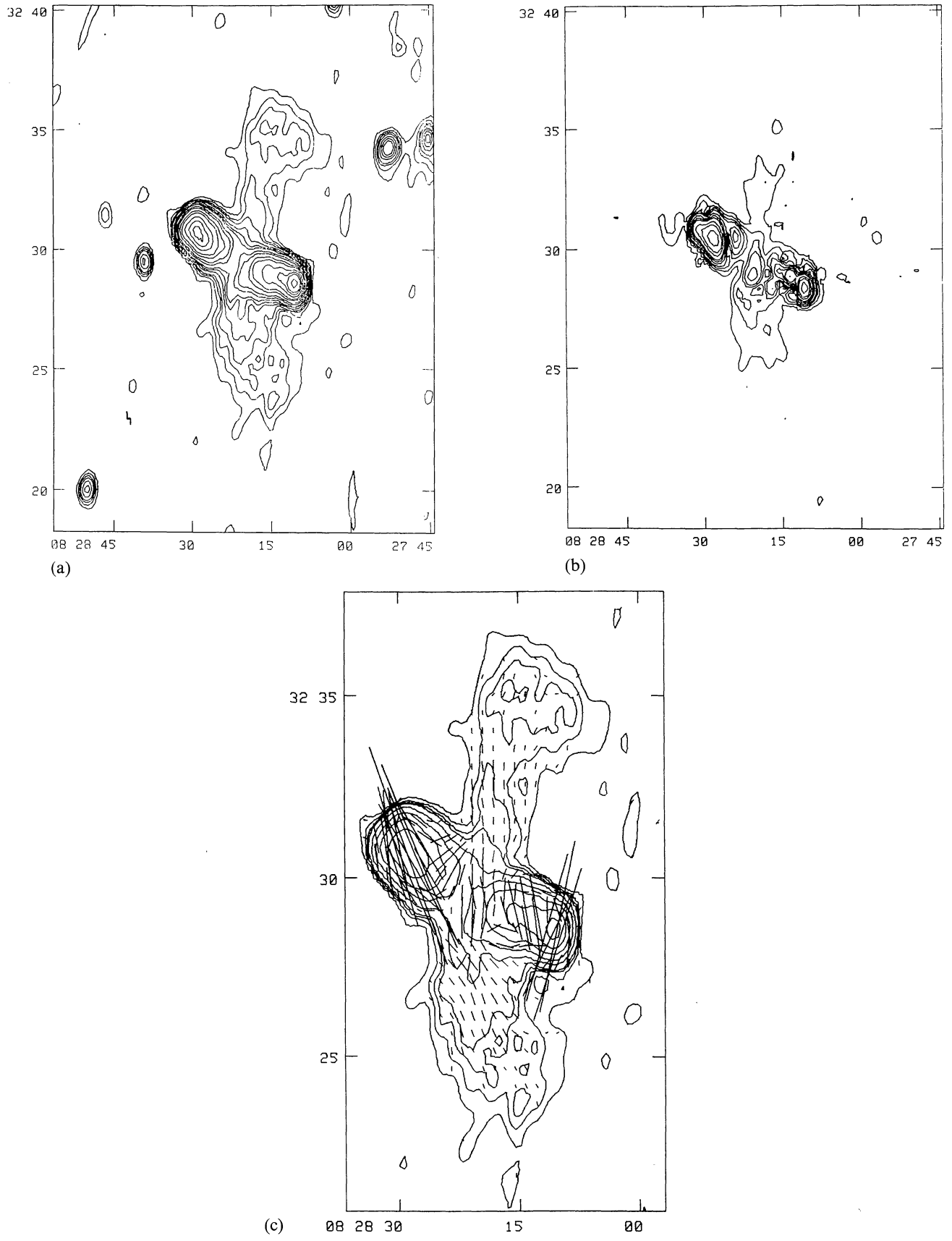

FIGURE 2. — Brightness distribution of B2 0828+32 at 0.6 GHz. (a) The total intensity map ; contours are : 2.5, 5, 7.5, 10, 15, 20, 25, 37.5, 50, 75, 100, 150, 200, 250, 375, 500 mJy/beam. (b) The polarized intensity map ; contours are : 2, 4, 6, 8, 12, 16, 20, 30, 40, 60, 80 mJy/beam. (c) Orientation of the projected magnetic field, superimposed to the 0.6 GHz total intensity contours.

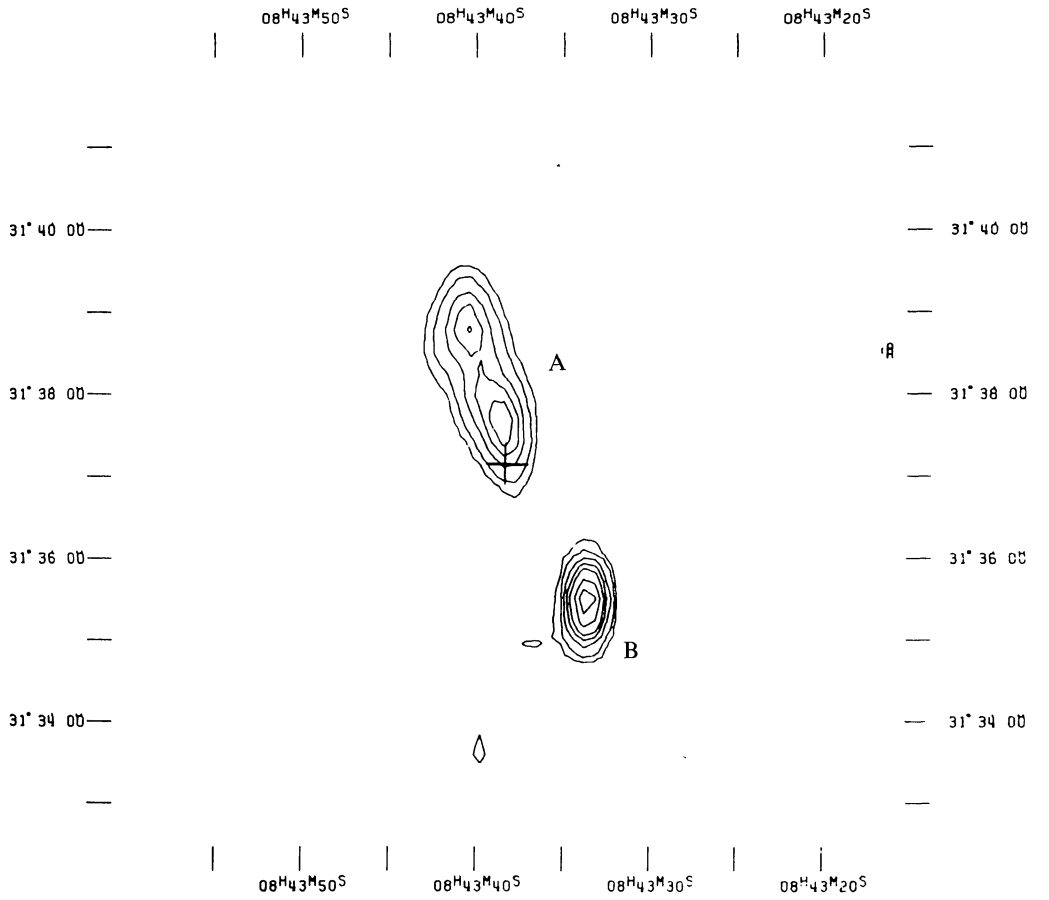

▲ FIGURE 3. — The total intensity brightness distribution of B2 0843+31 at 1.4 GHz. Contours are : 2.5, 5, 10, 15, 20, 30, 40 mJy/beam. The cross marks the position of the galaxy's center.

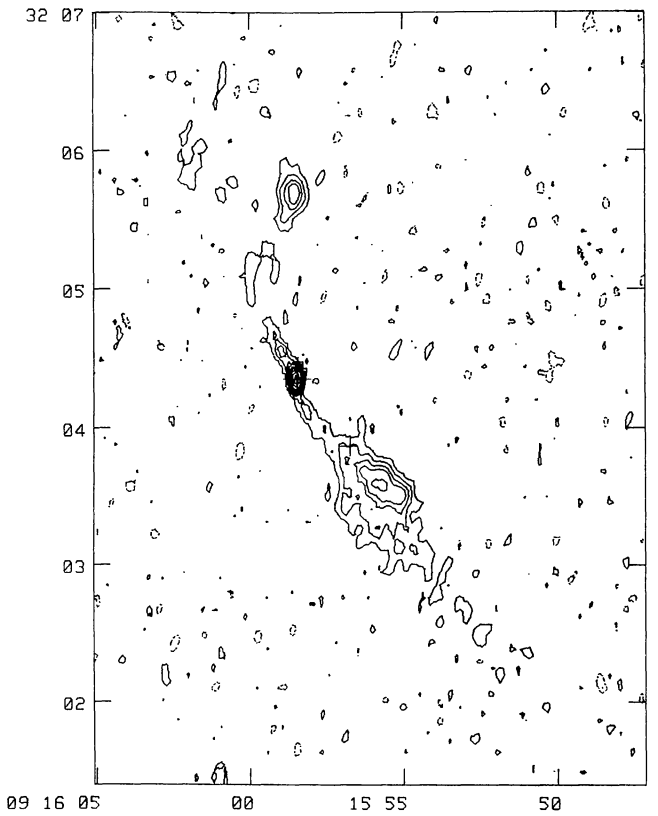

◀

FIGURE 4. — The total intensity brightness distribution of B2 0915+32 at 5.0 GHz ; contours are : 0.5, 1, 1.5, 2, 3, 4, 5, 7.5, 10 mJy/beam. The crosses mark the positions of the two galaxies.

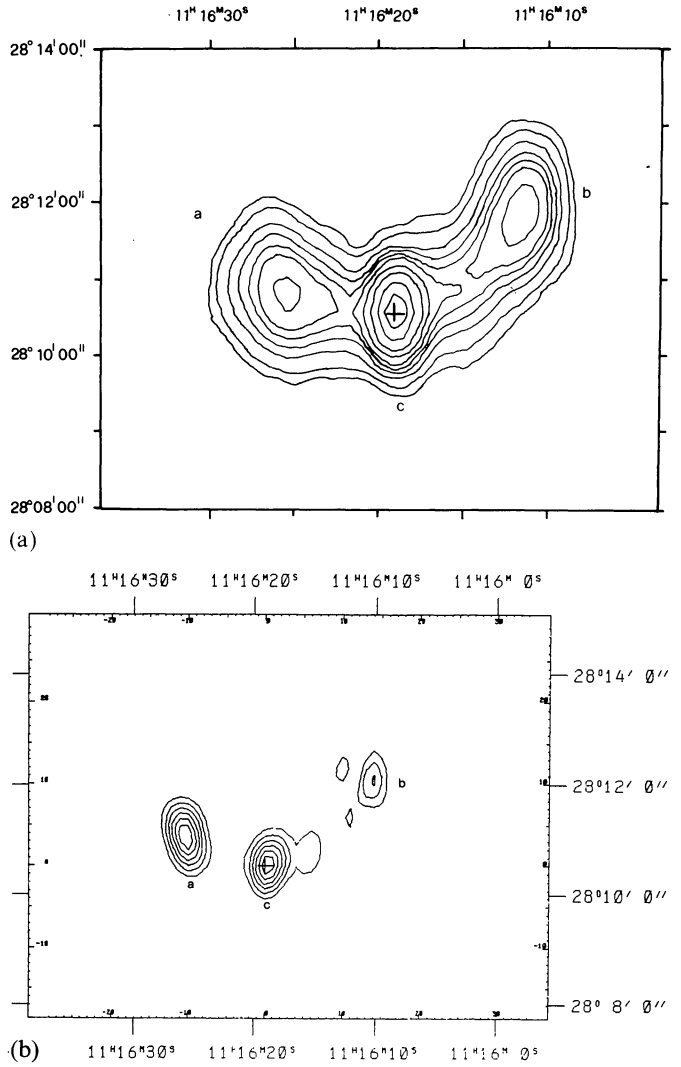

FIGURE 5. — The brightness distribution of B2 1116+28 at 1.4 GHz. The cross marks the position of the galaxy's center. (a) The total intensity map; contours are : 2.5, 5, 10, 15, 20, 25, 35, 50, 75, 100 mJy/beam. (b) The polarized intensity map; contours are : 2, 3, 4, 5, 6, 7 mJy/beam.

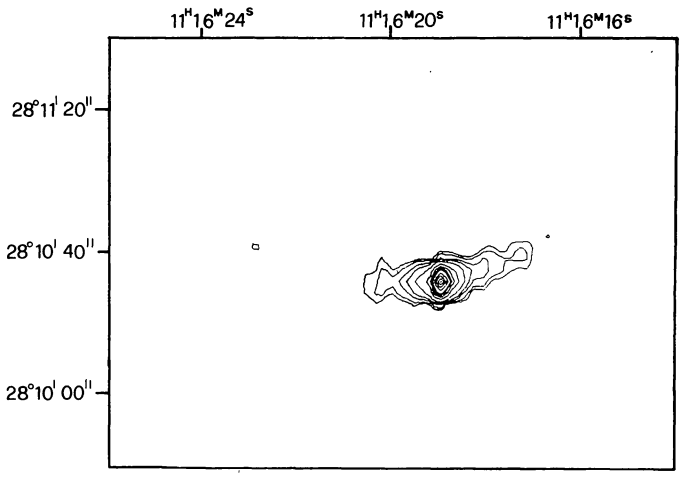

◀

FIGURE 6. — The total intensity brightness distribution of B2 1116+28 at 5 GHz. Contours are : 1, 1.5, 2.5, 3.5, 5.5, 9.5, 12.5, 15, 16.5, 20, 22.5, 25, 27.5, 30 mJy/beam. The cross marks the position of the galaxy's center.

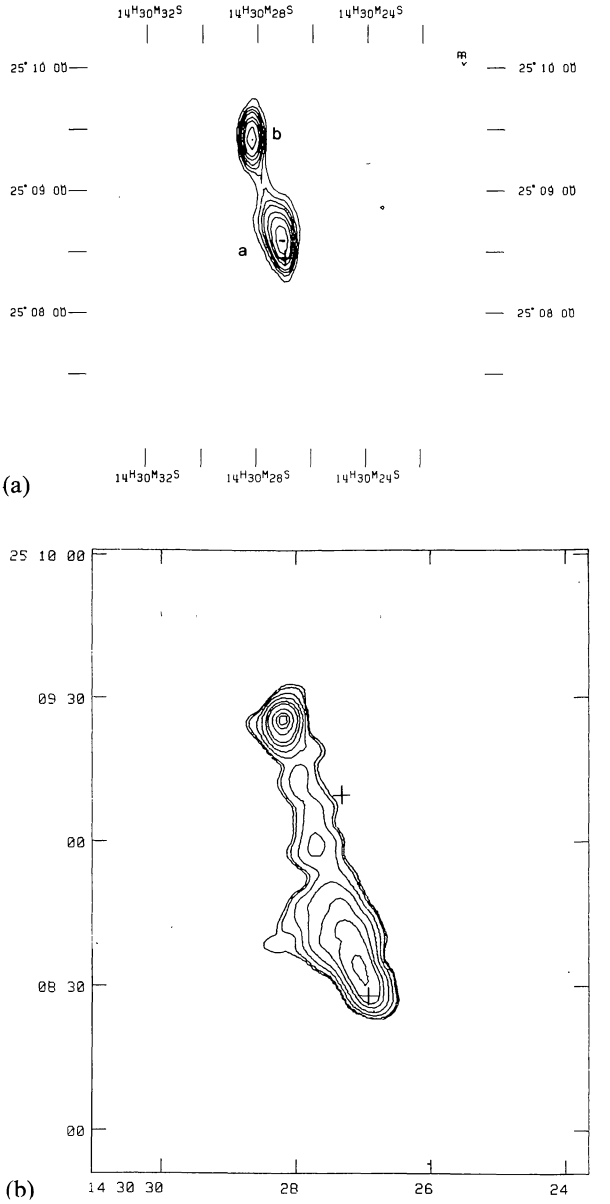

FIGURE 7. — (a) The total intensity brightness distribution of B2 1430+25 at 5 GHz. Contours are : 2.5, 5, 7.5, 10, 15, 20, 30, 40 mJy/beam. The cross marks the position of the galaxy's center. (b) The total intensity distribution at 1.4 GHz (VLA map). Contours are : 0.72 × (−1.5, 1.5, 2, 4, 8, 16, 25, 50, 75, 90) mJy/beam. The southern cross marks the optical position of the galaxy discussed in the text. The northern cross marks a fainter red object mentioned by Fomalont *et al.* (1978b), which seems unrelated to the source.

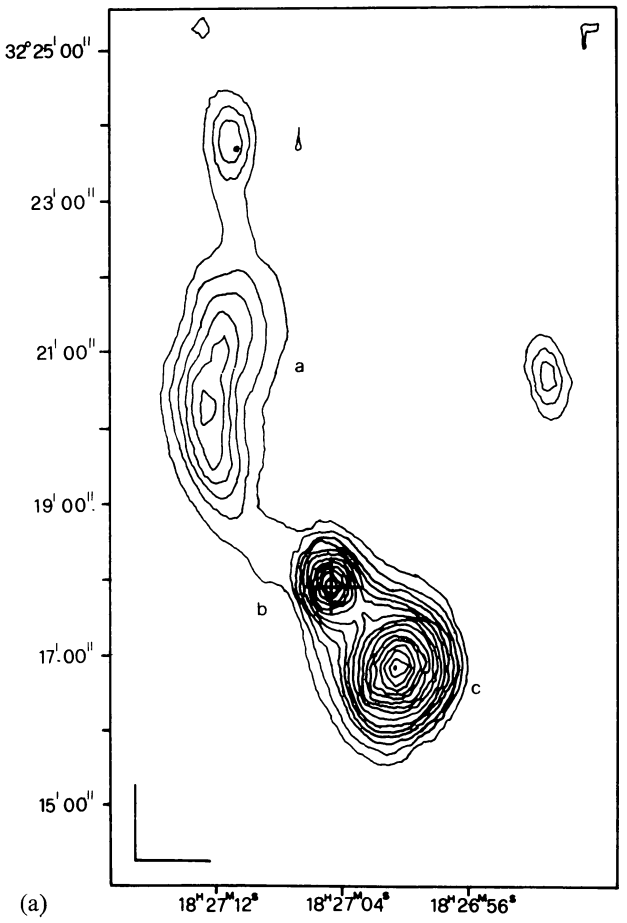

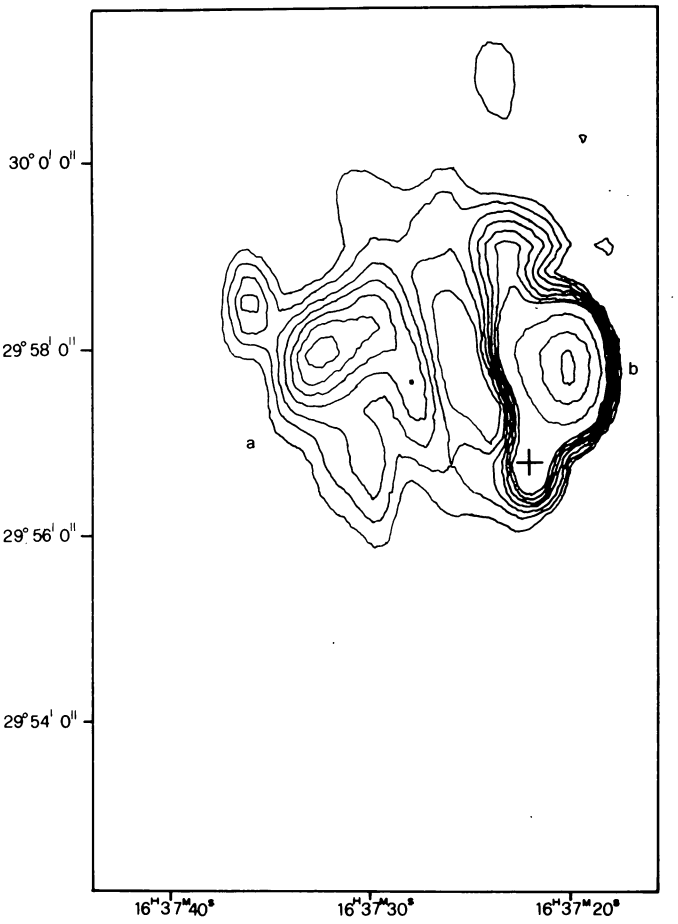

FIGURE 8. — The brightness distribution of B2 1637+29 at 1.4 GHz. The cross marks the position of the galaxy's center. The total intensity map; contours are : −1.5, 1.5, 3, 4.5, 6, 7.5, 9, 10.5, 25, 50, 75 mJy/beam.

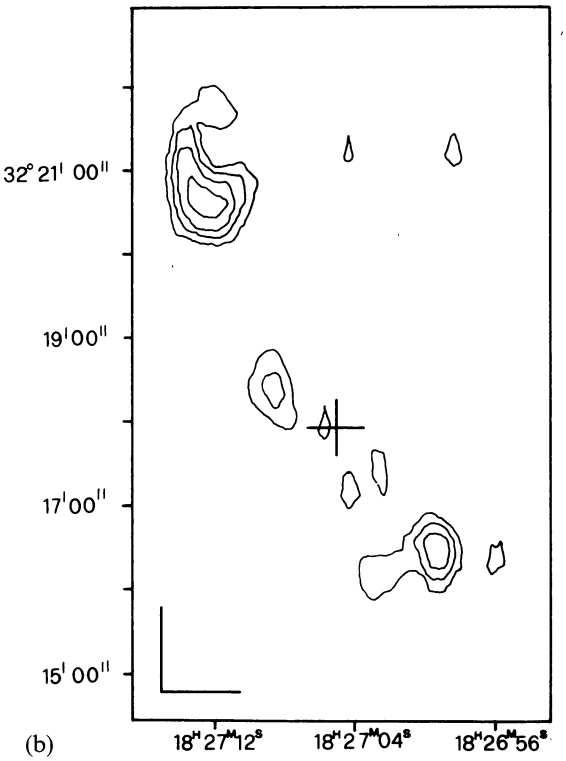

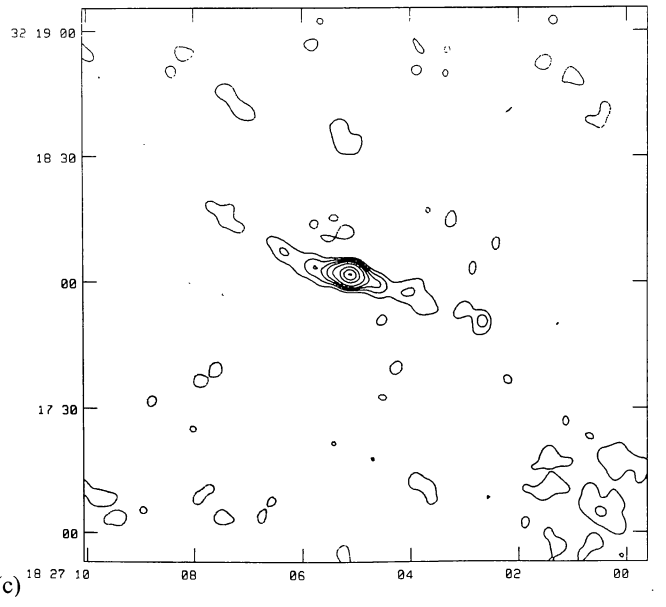

FIGURE 9. — The brightness distribution of B2 1827+32 at 1.4 GHz. The cross marks the position of the galaxy's center. (a) The total intensity WSRT map; contours are : 2.5, 5, 7.5, 10, ... mJy/beam. (b) The polarized intensity WSRT map; contours are : 1, 1.5, 2, 2.5 mJy/beam. (c) The total intensity VLA map of the central component; contours are : 0.2 × (− 3, 3, 6, 10, 15, 25, 50, 75, 99) mJy/beam.